AED R-3732F
Issued: April 10, 1971

Seventh Quarterly Report
Study to Determine and Improve Design for Lithium-Doped Solar Cells

Prepared for
Jet Propulsion Laboratory
California Institute of Technology
Pasadena, California
In fulfillment of
Contract No. 952555
January 1 to March 31, 1971

Prepared by
T. Faith, G. Brucker, and
A. Holmes-Siedle

RCA

RCA | Government and Commercial Systems
Astro Electronics Division | Princeton, New Jersey

AED R-3732F
Issued: April 10, 1971

Seventh Quarterly Report Study to Determine and Improve Design for Lithium-Doped Solar Cells

Prepared for
Jet Propulsion Laboratory
California Institute of Technology
Pasadena, California
In fulfillment of
Contract No. 952555
January 1 to March 31, 1971
Prepared by
T. Faith, G. Brucker, and
A. Holmes-Siedle

This work was performed for the Jet Propulsion Laboratory, California Institute of Technology, sponsored by the National Aeronautics and Space Administration under Contract NAS7-100.

RCA | Government and Commercial Systems
Astro Electronics Division | Princeton, New Jersey

ABSTRACT

This is the Seventh Quarterly Report on a program to study and analyze the action of lithium in producing a recovery or spontaneous annealing of radiation damage in bulk silicon solar cells. This program has technical continuity with the work performed by AED of RCA for JPL on Contract No. 952249. The goal of this effort is to understand the damage and recovery mechanisms so that an optimum set of solar-cell design rules can be specified.

The test vehicles used for this work are (1) a group of solar cells supplied by JPL, and (2) silicon bars in the "Hall-bar" configuration. The source of particle irradiation being used is a 1-MeV electron beam produced by the RCA Laboratories Van de Graaff generator. As called for in the contract, the Hall measurements terminated with the completion of the Fourth Quarterly Report. The solar cell testing will continue for the duration of the contract.

During the present reporting period, results have continued to point toward the lithium donor density gradient, dN_L/dw, as being the crucial parameter in the prediction of lithium cell behavior after irradiation by electrons. Recovery measurements on a large number (110) of oxygen-rich and oxygen-lean lithium cells fabricated by all three manufacturers have confirmed that cell recovery speed is directly proportional to the value of the lithium gradient for electron fluences ranging from 3×10^{13} e/cm^2 to 3×10^{15} e/cm^2. An approximate relationship between the time to half recovery, θ, (at room temperature) the lithium gradient, dN_L/dw, and the 1 MeV electron fluence Φ, was derived for oxygen-rich cells:

$$\theta \, dN_L/dw \approx 2.7 \times 10^{12} \, \Phi^{0.57} \text{ days/cm}^4,$$

which holds for the entire range of fluences tested. For oxygen-lean (Centralab and Heliotek) cells the relation

$$\theta \, dN_L/dw \approx 8.5 \times 10^{8} \, \Phi^{0.61} \text{ days/cm}^4$$

holds up to 1×10^{15} e/cm^2 above which a more rapid increase with fluence occurs, probably due to the greater significance of lithium depletion during irradiation. A similar relationship holds for oxygen-lean Texas Instruments cells, but with a proportionality constant approximately ten times that of the cells from the other manufacturers.

One hundred oxygen-rich (C13) cells with initial performance significantly above a group of commercial 10Ω-cm n/p cells were received recently. Seventy of these were irradiated to fluences ranging from 3×10^{13} to 3×10^{15} e/cm^2. Through

pre-irradiation capacitance measurements (giving dN_L/dw) and pre- and post-irradiation short-circuit current and diffusion length measurements, a relationship was derived between the diffusion length damage constant before recovery, $K_L(O)$, and dN_L/dw and Φ:

$$K_L(O) = 5.3 \times 10^{-18} (dN_L/dw)^{1/2} (1-0.063 \log_{10} \Phi).$$

The C13 cells are now recovering; when the recovery stage is complete a relation for the recovered damage constant $K_L(R)$ will be sought. Such a relation would enable complete description of the cell behavior in an electron environment in terms of the lithium gradient. Preliminary results on C13 cells that have completed recovery indicate less net damage than 10Ω-cm n/p cells, $K_L(R)$ at $\Phi = 1 \times 10^{14}$ e/cm^2 varying between 1.0×10^{-10} and 1.6×10^{-10} e^{-1} for the C13 cells compared to a 1.9×10^{-10} e^{-1} average for five 10Ω-cm n/p cells.

Gradient measurements have also been correlated with lithium diffusion schedules. Results have shown that long diffusion times ($\geq$ 5 hours) with a paint-on source result in large cell-to-cell variations in gradient, probably due to a loss of the lithium source with time. They also indicate that this problem can be overcome either by short diffusion times or by use of an evaporated lithium source.

Key results are as follows:

(1) The above work demonstrates that capacitance measurements may provide a quality control test that can be integrated into the production line or material acceptance activity.

(2) Damage constants for electron bombardment of lithium cells are becoming well-established

(3) As a result, prediction of cell performance and reliability in space is becoming a practical proposition.

TABLE OF CONTENTS

LIST OF ILLUSTRATIONS

LIST OF ILLUSTRATIONS (Continued

SECTION I

INTRODUCTION

A. GENERAL

This contract effort represents an experimental investigation of the physical properties of lithium-containing p-on-n solar cells and bulk silicon samples, and of the processes which occur in these devices and samples before and after irradiation. The program objectives are to develop and reduce-to-practice analytical techniques to characterize the radiation resistance of lithium-doped solar cells and its dependence on the materials and processes used to fabricate them. On the basis of these and other data, AED will determine and recommend an improved design of lithium-doped solar cells for space use. A previous RCA program (Contract No. 952249) performed for JPL provided the groundwork for this effort. Unless otherwise mentioned, the source of all irradiations was the 1-MeV electron beam of the RCA Laboratories Van de Graaff generator.

B. TECHNICAL APPROACH

The approach to the objectives is based on the irradiation and measurement of the electrical properties of bulk-silicon samples and government-furnished (GFE) solar cells. Experiments on bulk samples have included Hall and resistivity measurements taken as a function of: (1) bombardment temperature, (2) resistivity, (3) fluence, (4) oxygen concentration, and (5) annealing time at room temperature. Diffusion length and photovoltaic measurements and pre-irradiation capacitance measurements on solar cells are being made as a function of the same five parameters as for bulk samples. Stability studies are being conducted on solar cells, which have been irradiated and observed for long periods of time. Based on these results, a set of preliminary design rules and specifications have been determined, and solar cells are being procured by JPL in accordance with these rules. As a check of the validity of the design rules, tests will be conducted on this group of cells and a set of modified design rules will be derived.

C. SUMMARY OF PREVIOUS WORK

Some overall conclusions of previous reporting periods were as follows: the low-temperature measurements of Hall bars and of solar cells proved very successful and provided some fruitful insights into the processes occurring in

lithium-containing silicon. Correlation of lifetime damage constant K_τ with the carrier-removal rates, measured as a function of bombardment temperature ($\approx 80°K$ to $200°K$), was experimentally demonstrated.

Hall and resistivity measurements on samples of float-zone silicon doped with lithium to concentrations of 2 to 5×10^{14} Li/cm^3 and bombarded by electrons indicated the production of a defect located in the forbidden energy gap at an energy of 0.12 eV below the conduction band. This defect was produced at bombardment temperatures ranging from 78°K to 200°K. Annealing of these samples at a temperature of 100°C did not remove the defect completely, although the concentration was reduced. These lightly doped samples exhibited annealing properties and carrier-removal rates ($\Delta n/\Delta\phi = 0.1$ cm^{-1} at $T_B = 100°K$ to $200°K$) which are similar to those of heavily doped (2×10^{16} Li/cm^3) quartz-crucible Hall bar samples. The results of the Hall bar experiments suggested that the ratio of oxygen to lithium concentration is an important parameter in determining the annealing properties in lithium-doped silicon. These properties include the stability of both the lithium neutralized and unannealed defect centers, and also the carrier-removal rate for high bombardment temperatures ($T_B = 100°K$ to $200°K$). Defects located at an energy of $\approx E_C - 0.18$ eV and $\approx E_C - 0.13$ eV were measured in quartz-crucible silicon of moderate resistivity (2×10^{15} Li/cm^3) bombarded by electrons at temperatures from 78°K to 200°K. Both of these defects anneal at room temperature by the interaction of lithium with the defects. These defects would only influence the electrical characteristics of solar cells operating at room temperature if the lithium concentration in the cell was adjusted so as to locate the Fermi level within 2 kT of the defect energy level.

The rate of carrier-removal $(\Delta n/\Delta\phi \text{ cm}^{-1})_{SAT}$ appears to increase with decreasing lithium concentration. This suggests that the lithium combined with oxygen so as to limit the oxygen concentration available for A-center formation and the introduction rate of the LiOV center is lower than the A-center introduction rate.

Annealing results obtained on the quartz-crucible Hall bars suggest that several competing processes take place during the post-bombardment period. The short-term experimental results cannot be explained on the basis of a single or a double lithium ion neutralizing a defect. Over a long period of time following bombardment, the results can be explained as due to a multiple complexing by many lithium ions at a defect center so as to produce an uncharged complex.

Cold finger experiments were performed on oxygen-lean cells and on quartz-crucible cells with a wide range of lithium density gradients. Bombardment temperature, T_B, dependence of lifetime damage constant, K_τ, was measured. Both types of cells displayed a saturation of K_τ at high T_B and a decrease at lower temperatures in agreement with results previously obtained from carrier removal experiments on Hall samples. K_τ saturated at $T_B = 100°K$ to $120°K$.

The lifetime damage constant for $T > 120°K$ is a factor of ≈ 5 higher in oxygen-lean lithium cells than in crucible (Li) cells.

Recovery rate measurements versus annealing temperature showed the activation energy for recovery in several groups of crucible cells to be ≈ 1.1 eV, which is the activation energy for lithium diffusion in crucible-grown silicon, and that for several groups of oxygen-lean cells to be ≈ 0.65 eV, the activation energy for lithium diffusion in silicon with low-oxygen content.

Diffusion constant measurements made on quartz-crucible cells show an activation energy of 1.03 eV indicative of dissociation of LiO^+ and diffusion of Li^+.

Performance tests on the solar cells showed that most of the lithium cells from recent shipments had initial powers greater than the commercial n/p cells. The pre-irradiation lithium donor density gradient, dN_L/dw, provides a good index of the lithium density distribution near the junction and of the dynamic behavior of cell, the cell recovery rate being directly proportional to the lithium gradient.

Long-term stability tests at room temperature on lithium-containing crucible-grown cells continued to show these cells to be stable. Most of the crucible cells which have completed their recovery cycles were competitive in power with commercial 10 ohm-cm n/p cells irradiated to the same fluence. For a fluence of 3×10^{14} e/cm^2, the time-to-half-recovery, θ, of these cells was related to the lithium density gradient dN_L/dw, through $\theta\, dN_L/dw = 6.5 \pm 2.5 \times 10^{20}$ days/cm^4 for $10^{18} \leqslant dN_L/dw \leqslant 5 \times 10^{19}$ cm^{-4}. Oxygen-lean cells with heavy lithium doping ($dN_L/dw \gtrsim 10^{19}$ cm^{-4}) have suffered some form of instability, either post-recovery redegradation or instability independent of irradiation. The post-recovery short-circuit current redegradation was the most common instability. However, cells which suffered this instability did stabilize after a ≈ 100 day redegradation period. A radiation independent open-circuit voltage instability was suffered by cells of lots C4 and C5. This loss, which is due to carrier loss in the base region, has occurred continuously over ≈ 500 days.

SECTION II

PARAMETRIC STUDIES OF LITHIUM CELLS

A. GENERAL

The principal performance parameters characterizing lithium cell behavior in a radiation environment are (1) the initial (pre-irradiation) performance levels (2) the rate of cell degradation or damage constant (3) cell recovery rate versus cell temperature and (4) final photovoltaic performance after recovery from a given fluence. Under the present contract, experiments on solar cells irradiated by 1 MeV electrons have been designed with the aim of eventually relating the above performance parameters and the manufacturers' fabrication parameters to a set of physical parameters obtainable through non-destructive measurements on unirradiated cells. This would provide the cell manufacturers with (1) the optimum set of fabrication parameters for a given cell application, and (2) a set of quality-control tests that can be integrated into the production line.

In earlier work on this contract the dependence of recovery rate on cell temperature was obtained for both oxygen-rich and oxygen-lean lithium cells through measurements of activation energy for diffusion-length recovery (Reference 1). For a given cell temperature, the recovery rate of short-circuit current in the 10^{14} e/cm^2 fluence range was shown to vary linearly with the lithium density gradient (Reference 2) for both oxygen-rich and oxygen-lean cells. In the work of the present reporting period, (1) recovery rate versus lithium gradient measurements were extended to cover the fluence range from 3×10^{13} to 3×10^{15} e/cm^2; (2) a relationship between diffusion-length damage constant, K_L, lithium gradient, dN_L/dw, and 1 MeV electron fluence, Φ, was obtained through measurements on seventy irradiated cells of lot C13, and (3) pre-irradiation capacitance measurements on one hundred C13 cells established relationship between fabrication parameters (temperature and time of lithium diffusion) and the degree of control of the lithium density gradient, dN_L/dw, near the junction.

B. INITIAL CELL PERFORMANCE

A shipment of one hundred high performance lithium cells fabricated from quartz-crucible silicon (lot C13) were received from JPL during the present reporting period. They consisted of ten groups (C13A to C13J), ten cells per group, with the parameters varied between groups being lithium diffusion temperature and diffusion time. Lithium density gradients, dN_L/dw, were obtained from reverse-bias capacitance measurements on all of the C13 cells. Some of

the individual groups showed large cell-to-cell variations in gradient. This finding and its relationship to the individual cell groups will be discussed further in section IIE; in this section the cells are divided into three batches according to lithium gradient, without distinctions between groups. The three photovoltaic parameters, maximum power, P_{max}; short-circuit current, I_{SC}; and open-circuit voltage, V_{OC}, are plotted in Figures 1, 2 and 3 respectively. For these figures the cells were divided into batch 1, consisting of 20 cells with gradient ranging from 0.65×10^{18} to 3.3×10^{18} cm^{-4}; batch 2, with 40 cells ranging from 3.3×10^{18} to 9.0×10^{18} cm^{-4}; and batch 3, with 40 cells ranging from 9.0×10^{18} to 1.6×10^{19} cm^{-4}. *

The data points appear along the absicca at the average value of dN_L/dw for the batch and the five ordinates represent (from top to bottom) the highest value, the values exceeded by 20, 50, and 80 percent of the cells, and the lowest value for the batch. Equivalent values for a batch of 20 commercial 10 Ω-cm n/p cells are shown on the left in each figure. The general trends show the power and short-circuit current to remain approximately constant over the first two batches, then drop with batch 3, while the open-circuit voltage increases monotonically with gradient. The maximum power of all lithium batches exceeds that of the n/p batch, most of this advantage being due to the higher V_{OC} which is due in turn to the heavier base doping in the lithium cells.

C. DAMAGE CONSTANT

Seventy of the C13 cells were irradiated with 1 MeV electrons; seventeen cells to a fluence of 3×10^{13} e/cm^2, nine to 1×10^{14} e/cm^2, twenty to 3×10^{14} e/cm^2, eight to 1×10^{15} e/cm^2, and sixteen to 3×10^{15} e/cm^2. The cells were chosen so that seven cells from each group were irradiated, and so that the cells irradiated to 3×10^{13} e/cm^2, 3×10^{14} e/cm^2 and 3×10^{15} e/cm^2 covered the widest possible range of lithium gradients. Room-temperature photovoltaic characteristics under 140 mW/cm^2 tungsten illumination were taken on all cells immediately after irradiation. The cells were then stored at 80° C to recover.

A number of interesting results were obtained from the short-circuit current readings made immediately after irradiation (before recovery). This current is plotted in Figure 4 versus lithium donor density gradient, dN_L/dw, for the

---

* Batch 1 has the smaller number of cells because of the comparatively small fraction of cells in the low gradient range.

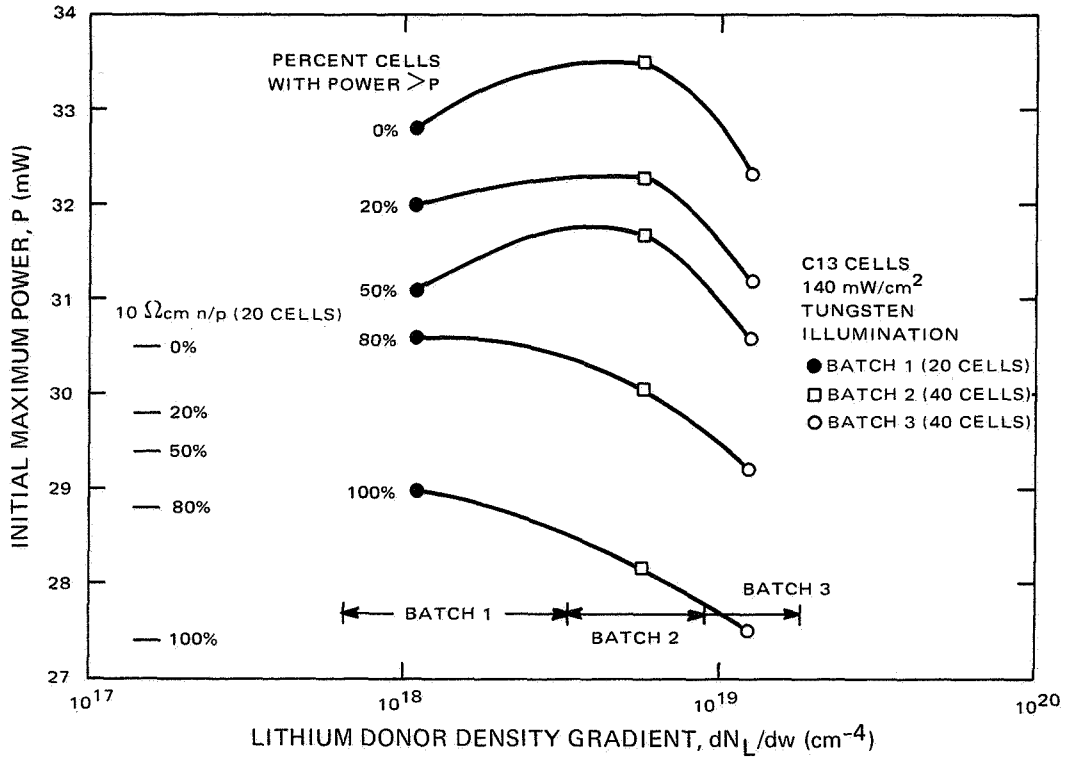

Figure 1. Initial Maximum Power Distributions for C13 Quartz-Crucible Lithium Cells versus Lithium Donor Density Gradients with Comparisons of 10Ω-cm Commercial n/p Cells

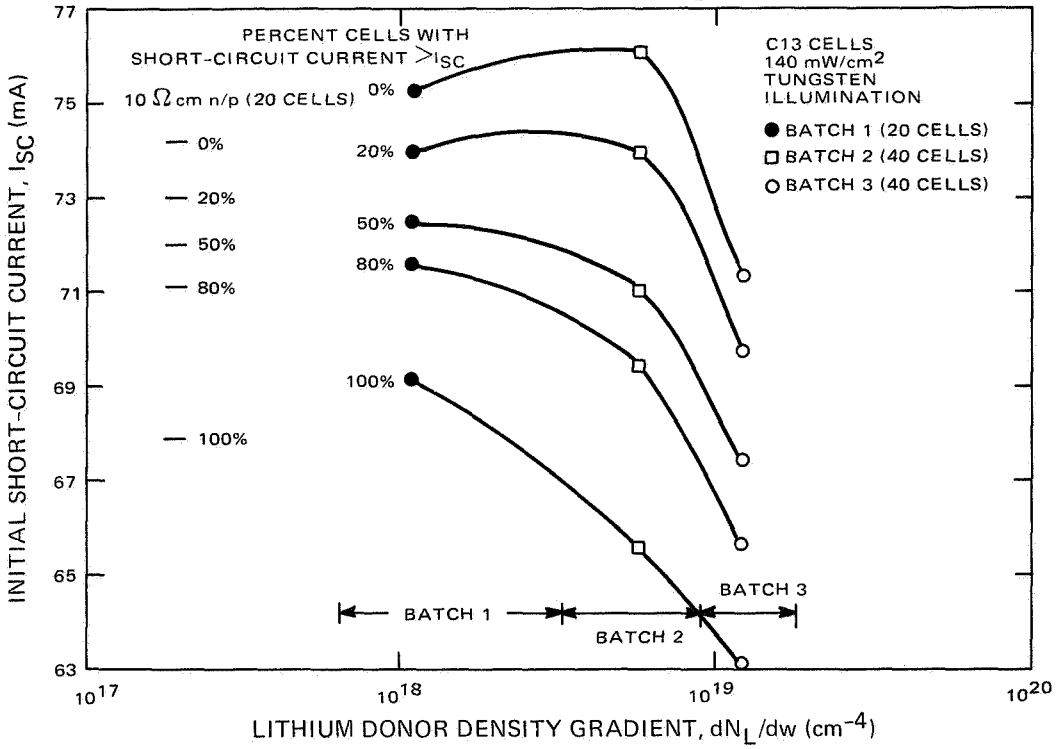

Figure 2. Initial Short-Circuit Current Distributions for C13 Quartz-Crucible Lithium Cells versus Lithium Donor Density Gradients with Comparisons of 10Ω-cm Commercial n/p Cells

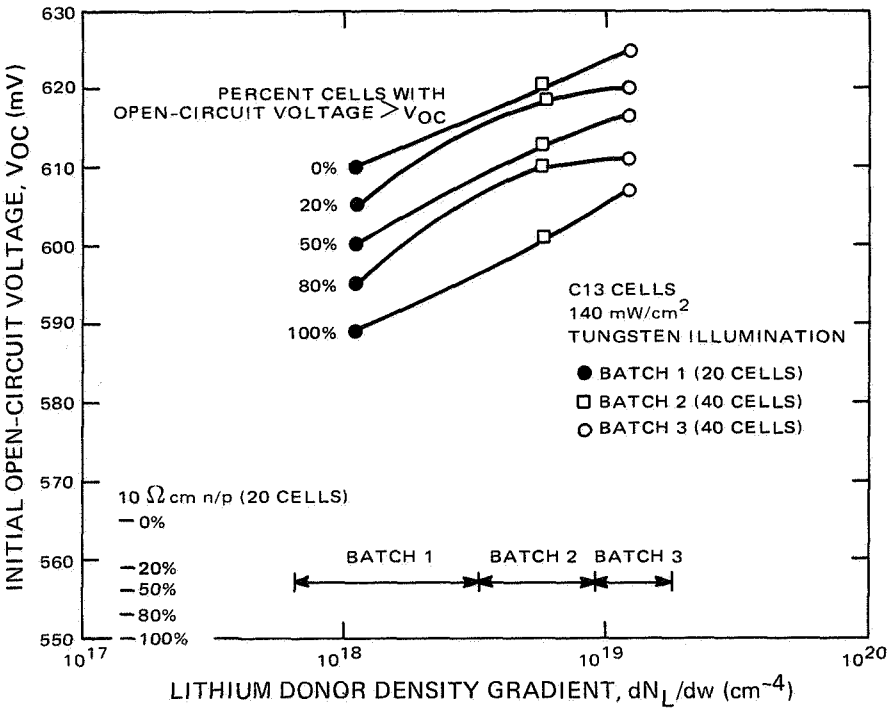

Figure 3. Initial Open-Circuit Voltage Distribution for C13 Quartz-Crucible Lithium Cells versus Lithium Donor Density Gradients with Comparisons of 10Ω-cm Commercial n/p Cells

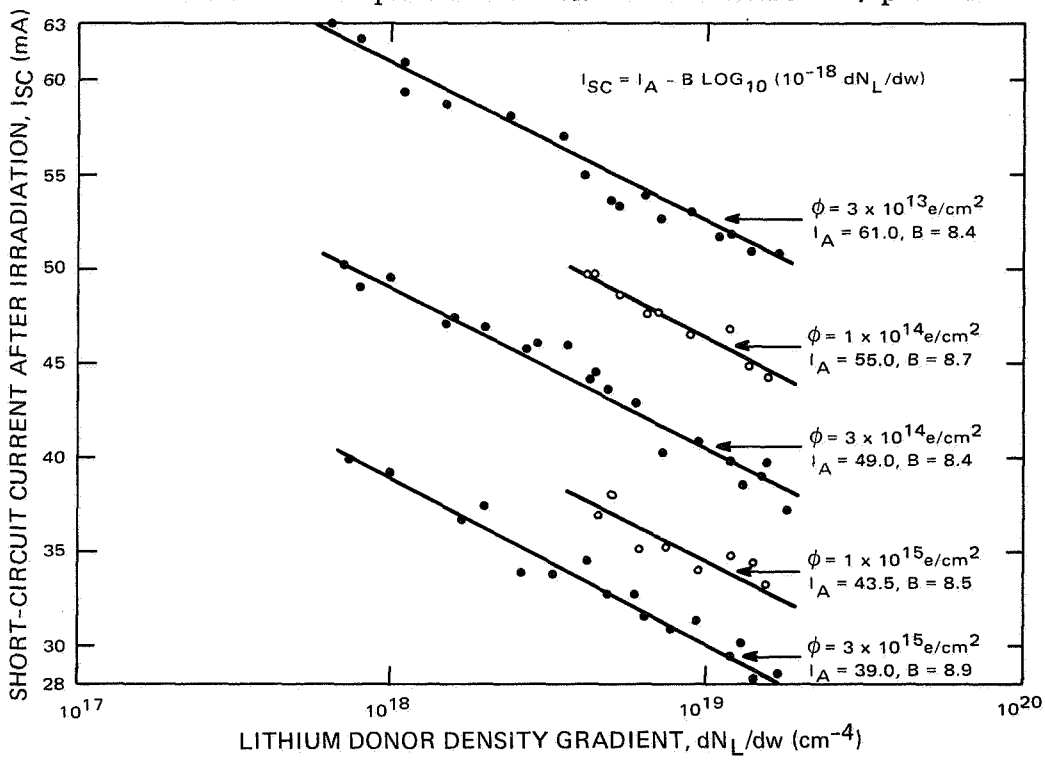

Figure 4. Short-Circuit Current Immediately after Irradiation versus Lithium Density Gradient for Seventy C13 Cells Irradiated by 1 MeV Electrons to Fluences Ranging from 3×10^{13} e/cm^2 to 3×10^{15} e/cm^2

seventy irradiated cells. Within the scatter of the data, the points at each fluence fit well along a straight line, all five lines having approximately the same slope. A best least-squares fit to the equation

$$I_{SC} = I_A - B \log_{10} (10^{-18}\, dN_L/dw), \tag{1}$$

was calculated for each fluence.

The values of B were found to be 8.4, 8.7, 8.4, 8.5 and 8.9 for $\phi = 3 \times 10^{13}$, 1×10^{14}, 3×10^{14}, 1×10^{15}, and 3×10^{15} e/cm^2, respectively. These equations give a specific relation between the amount of initial damage (before recovery) and the lithium gradient in crucible-grown cells. It is advantageous to describe this damage in terms of a more standard quantity, namely the diffusion-length damage constant before recovery, $K_L(O)$, given by

$$K_L(O)\, \Phi = \frac{1}{L(O)^2} - \frac{1}{L_O^2}, \tag{2}$$

where L_O and $L(O)$ are the diffusion lengths in the base region of the cell before irradiation and immediately after irradiation, respectively. To obtain $K_L(0)$, the relationship between I_{SC} and L must be known; Figure 5 gives such a plot for C13 cells. The data for this figure was generated from simultaneous short-circuit-current and diffusion length* measurements made on all of the C13 cells, 30 of which were unirradiated, the other 70 being at various stages of recovery after irradiation. The best fit to this data is

$$I_{SC} = 34.4 \log_{10} L. \tag{3}$$

For fluences above 3×10^{13} e/cm^2, $1/L(O)^2 >> 1/L_O^2$ in equation (2) and the latter term can be dropped with less than 10 percent error. This approximation, combining equations (1), (2) and (3), and using B = 8.6 in equation (1), gives

$$K_L(O) = \frac{10^{-(1 + I_A/17.2)}}{\Phi} \sqrt{\frac{dN_L}{dw}}, \tag{4}$$

which is valid for all of the fluences employed except $\Phi = 3 \times 10^{13}$ e/cm^2. For this lowest fluence $K_L(O)$ was calculated taking L_O into account. The result, which is shown in Figure 6, was

$$K_L(O) = 8.5 \times 10^{-19} \sqrt{dN_L/dw}. \tag{5}$$

---

* Obtained from measurements using band-gap light that was calibrated with the electron-voltaic method using 15 different lithium and n/p solar cells.

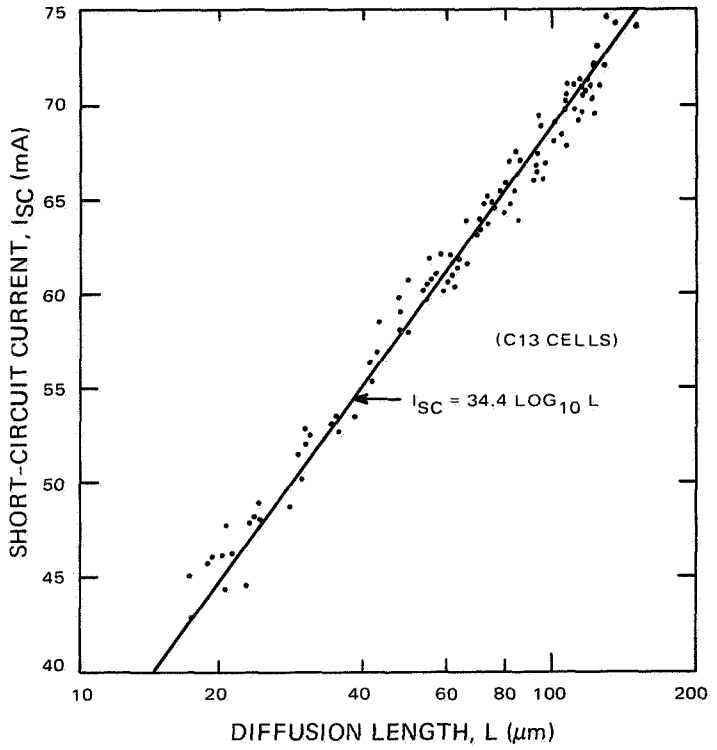

Figure 5. Short-Circuit Current versus Diffusion Length for 100 Crucible (C13) Cells; 30 Cells Unirradiated, 70 Cells at Various Stages of Recovery after Irradiation

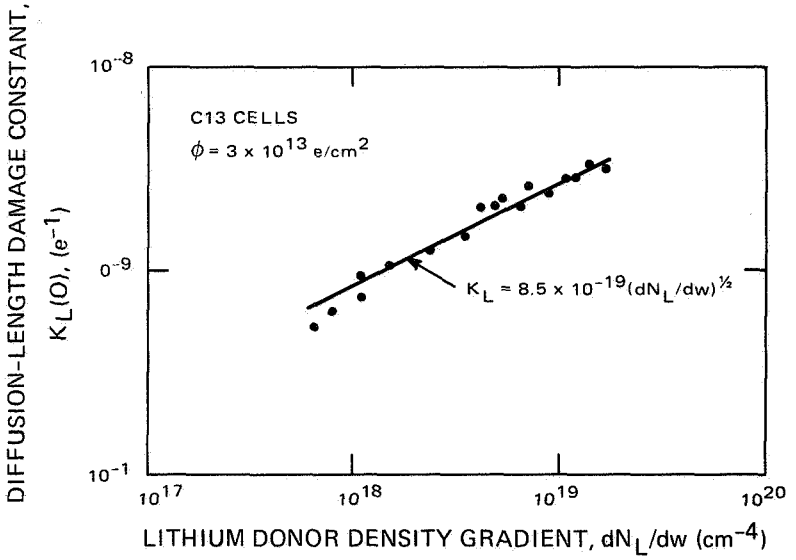

Figure 6. Diffusion-Length Damage Constant Immediately After Irradiation, i.e., Before Recovery, versus Lithium Gradient for Seventeen C13 Cells Irradiated to a Fluence of 3×10^{13} e/cm^2

Equations (4) and (5), together with the appropriate values of I_A listed in Figure 4, give the fluence dependence of $K_L(O)$, which is plotted in Figure 7 for $dN_L/dw = 10^{18}$ cm^{-4}. Figure 7 shows a logarithmic dependence on fluence described (for $dN_L/dw = 10^{18}$ cm^{-4}) by

$$K_L(O) = 5.3 \times 10^{-9} (1 - 0.063 \log_{10} \Phi). \quad (6)$$

Inserting the lithium gradient dependence, the expression for K_L as a function of Φ and dN_L/dw is given by

$$K_L(O) = 5.3 \times 10^{-18} (dN_L/dw)^{1/2} (1 - 0.063 \log_{10} \Phi). \quad (7)$$

The applicability of this relationship to other crucible cells was tested using the post-irradiation data on thirteen previously irradiated cells from lot H3A. These H3A cells covered a wide range of gradients: $3 \times 10^{17} \leq dN_L/dw \leq 1.3 \times 10^{19}$ cm^{-4}; they were irradiated to a fluence of 3×10^{14} e/cm^2. Figure 8 shows $K_L(O)$ plotted against dN_L/dw for these cells. The square-root dependence on gradient is evident, the best least-squares fit being obtained with the relationship

$$K_L(O) = 4.4 \times 10^{-19} (dN_L/dw)^{1/2}. \quad (8)$$

This is within 10 percent of the value of $4.8 \times 10^{-19} (dN_L/dw)^{1/2}$ obtained for the C13 cells, as can be seen in Figure 7, where the H3A data point is shown together with the C13 data.

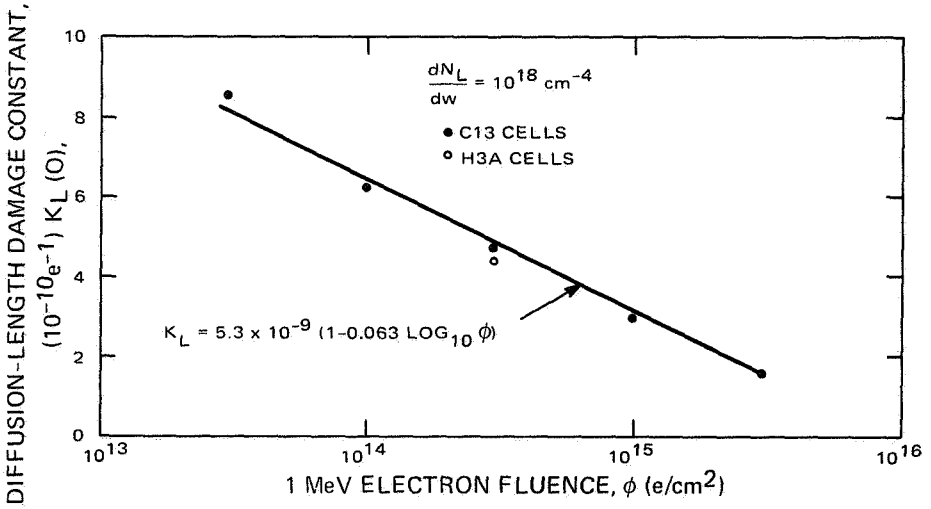

Figure 7. Diffusion-Length Damage Constant Immediately after Irradiation (at $dN_L/dw = 10^{18}$ cm^{-4}) versus 1 MeV electron fluence; C13 and H3A Cells

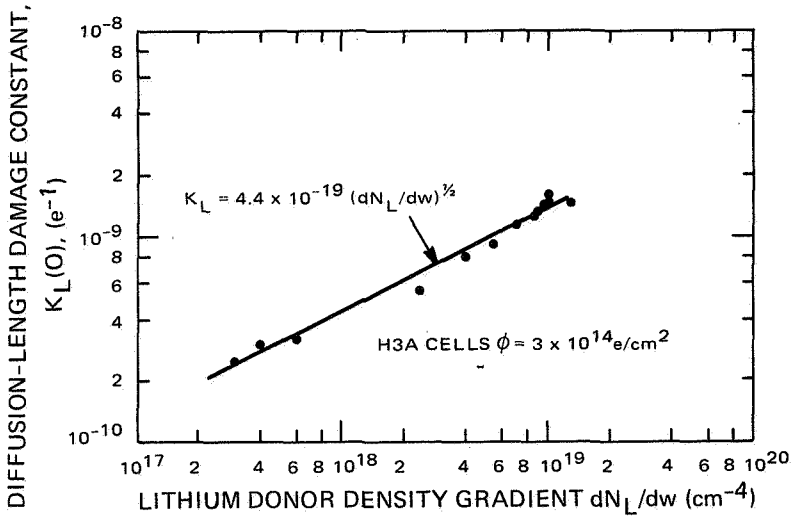

Figure 8. Diffusion-Length Damage Constant Immediately after Irradiation versus Lithium Gradient for H3A Cells Irradiated to a Fluence of 3×10^{14} e/cm^2

The C13 cells are now recovering at 80° C. At completion of short-circuit current recovery, the effective damage constant, $K_L(R)$, after cell recovery can be computed from

$$K_L(R)\,\Phi = \frac{1}{L(R)^2} - \frac{1}{L_0^2} \qquad (8)$$

where L(R) is the diffusion length after recovery. There is a large uncertainty in $K_L(R)$ for low fluences since $I(R) \sim I_0$. Results at 3×10^{13} e/cm^2 show a very large scatter, $K_L(R)$ ranging from 0.5×10^{-10} to 2.0×10^{-10} e^{-1}. The results at 1×10^{-14} e/cm^2 are more coherent and show a slight increase with lithium gradient, $K_L(R)$ ranging from 1.0×10^{-10} to 1.6×10^{-10} e^{-1} for gradients ranging from 4×10^{18} to 1.6×10^{19} cm^{-4}. For comparison, similar results on five 10Ω-cm n/p cells irradiated to 1×10^{14} e/cm^2 yielded a damage constant, averaged over the group, of 1.9×10^{-10} e^{-1}, a higher value than that of the lithium cells, indicating heavier net damage in the n/p cells. Most of the lithium cells irradiated to higher fluences are still recovering, so the damage constant results at this stage are still preliminary. A future experiment is planned in which the thirty remaining (unirradiated) C13 cells will be irradiated to a series of fluences together with a large group of n/p cells. Damage constants before and after recovery will be obtained from direct diffusion-length measurements on the individual cells.

D. RECOVERY CHARACTERISTICS

Many of the C13 cells are still in their recovery stage, so complete recovery data is not yet available on these cells.

Prior to the tests on the C13 cells, a large number of previously unirradiated oxygen-lean cells from past shipments were gathered and irradiated to fluences ranging from 3×10^{13} e/cm^2 to 3×10^{15} e/cm^2. Cells from Texas Instruments, Heliotek and Centralab* of both Lopex** and Float-Zone silicon were represented. They included a wide range of diffusion schedules and initial performance levels. After irradiation, short-circuit current was measured as a function of time on all of the cells. The purpose of the experiment was to test the validity of the previously observed (Reference 2) linear relationship between recovery speed and lithium density gradient for a large batch of cells covering the widest possible range of lithium gradients and a wide range of fluences.

A typical short-circuit current versus time curve during recovery is shown in Figure 9. The time to half recovery, θ, defined by

$$\frac{I(R) - I(\theta)}{I(R) - I(O)} = 0.5, \qquad (9)$$

where I(R) is the short-circuit current at peak recovery, provides the most well-defined index of (inverse) recovery rate. For the cell in Figure 9, $\theta = 55$ minutes (or 0.038 days). The values of θ for the Centralab and Heliotek cells are plotted against lithium density gradient in Figure 10 for four fluences ranging from 3×10^{13} to 3×10^{15} e/cm^2. Included are all the cells tested from these manufacturers except those of lots C4 and C5 and those with lithium gradients greater than 10^{20} cm^{-4}. The points on these logarithmic plots fit remarkably well along straight lines with minus one slope, confirming the linear relationship between recovery speed and lithium gradient. The θ dN_L/dw products (averaged over the cells at each fluence) are: 1.7×10^{17} days/cm^4 for 3×10^{13} e/cm^2; 3.4×10^{17} days/cm^4 for 1×10^{14} e/cm^2; 7.2×10^{17} days/cm^4 for 3×10^{14} e/cm^2, and 6.8×10^{18} days/cm^4 for 3×10^{15} e/cm^2. There are two cell lots that do not follow these curves, lots C4 and C5, which recover at a faster rate than the curves predict. However, these two lots had already been identified as mavericks in previous work (Reference 2), having been shown to suffer open-circuit voltage instability due to a decrease in lithium gradient with time. In addition, cells with gradients greater than 10^{20} cm^{-4} (C10C and C10F cells)

---

* Lots T3, T4, T5, T6, T7, T9, T10, H5, H7, H1A, H5A, H7A, H (NASA-furnished in 1967), C4, C5, C8F, C10C, C10F, and C11C were represented.

** Trademark of Texas Instruments Corporation

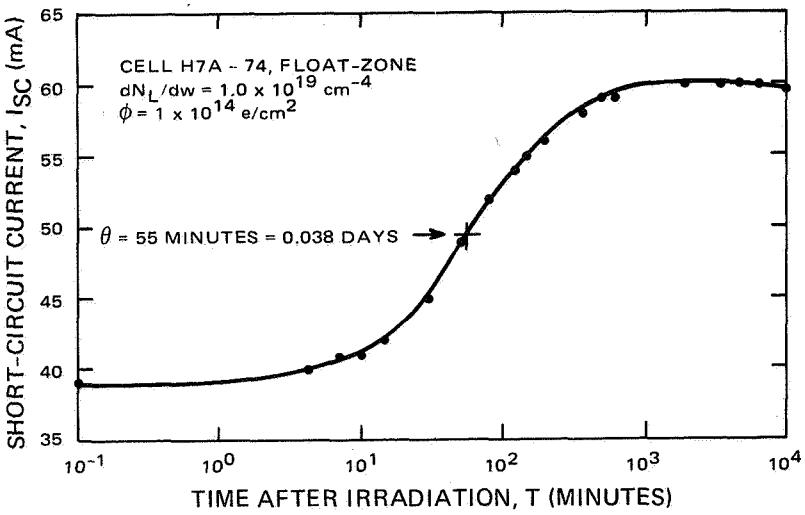

Figure 9. Typical Short-Circuit Current Recovery Curve Illustrating the Index of Cell Recovery Rate, θ, used in Subsequent illustrations

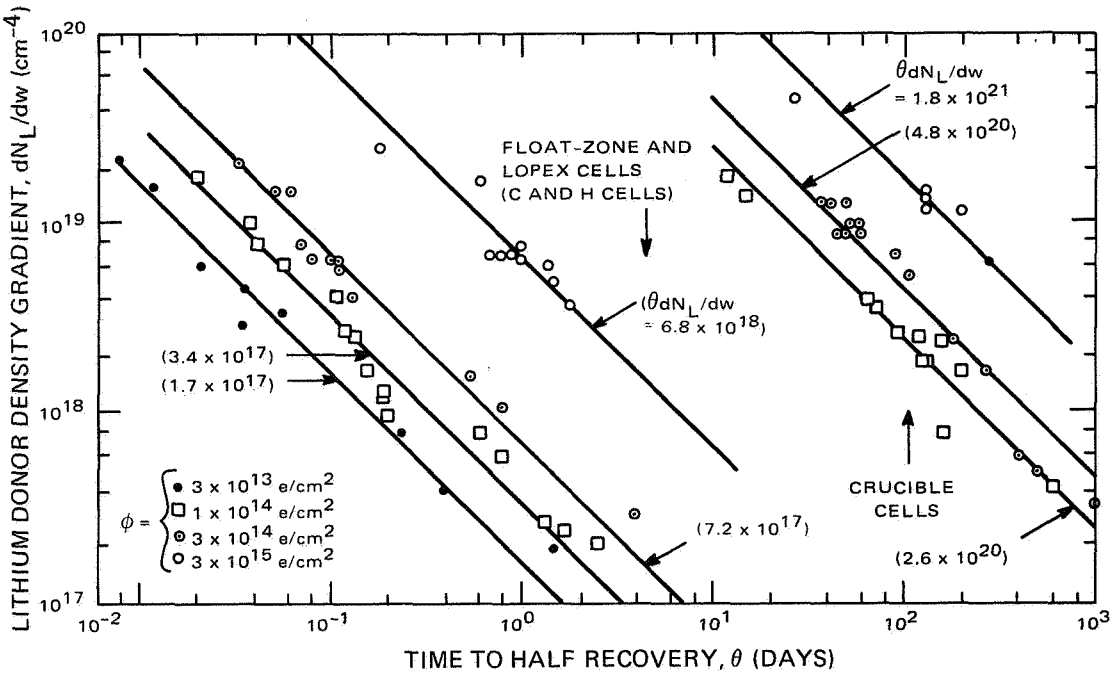

Figure 10. Time to Half Recovery at Room Temperature versus Lithium Gradient, for Oxygen-Rich Cells and for Centralab and Heliotek Oxygen-Lean Cells Irradiated to Fluences Ranging from 3×10^{13} to 3×10^{15} e/cm^2

recovered more slowly at low fluence than predicted by the curves. A feasible explanation for this is that the gradient in these cells is not a good index of the average lithium density near the junction. The capacitance measurements give evidence of this in the form of a leveling off of the lithium density; i.e., a decrease in gradient, at distances of less than 1 micrometer from the junction for cells with $dN_L/dw > 10^{20}$ cm^{-4}.

Curves of θ versus dN_L/dw for oxygen-rich crucible cells are shown in the upper portion of Figure 10. The data are drawn from previous results on cells that recovered at room temperature, 60° C, or 80° C. [In the latter two cases equivalent recovery time at room temperature was calculated using the activation energy previously obtained (Reference 1) for crucible cell recovery.] At 1×10^{14} e/cm^2 and 3×10^{14} e/cm^2 the separation between the oxygen-lean (FZ and L) curve and the crucible curve is $\approx$ 700, which is approximately the ratio of the room-temperature lithium diffusion constant in oxygen-lean silicon to that in oxygen-rich silicon. However, at the highest fluence, 3×10^{15} e/cm^2, the separation is only $\approx$ 250. This suggests that lithium is lost more rapidly in defect formation in oxygen-lean cells than in oxygen-rich cells, supporting previous carrier removal observations (Reference 3) in bulk-sample measurements.

A puzzling anomaly was observed in the case of the oxygen-lean T cells. While the constancy of the $\theta\ dN_L/dw$ product was satisfied by these cells at each fluence as shown in Figure 11, the products were approximately an order of magnitude higher than the equivalent products for the Centralab and Heliotek cells. This can be seen by comparing the products in Figure 11 with those of Figure 10. This discrepancy is not understood at present. One of the main differences between the manufacturers is that the TI cells have used an evaporated lithium source whereas all of the oxygen-lean C and H cells tested to date have used a paint-on source. It would seem likely that a difference in silicon type would cause differences in recovery rate. This would be particularly feasible for Lopex versus float-zone recovery since the oxygen-content is generally higher in Lopex silicon. However, as was shown in Figure 10, the same recovery rate applies for both Lopex and float-zone C and H cells. Dislocation counts are now being made on some of the cells in an effort to confirm the silicon types employed.

The approximate linear dependence of recovery speed on lithium gradient at all the fluences tested enables prediction of the recovery speed of any lithium cell with lithium gradient between 10^{17} and 10^{20} cm^{-4} in this fluence range. This is illustrated in Figure 12, which gives plots of the $\theta\ dN_L/dw$ products of all the cells tested versus 1 MeV electron fluence.

Below 10^{15} e/cm^2 this product increases gradually with fluence in all types of cells. In oxygen-lean cells there is a more pronounced dependence on fluence

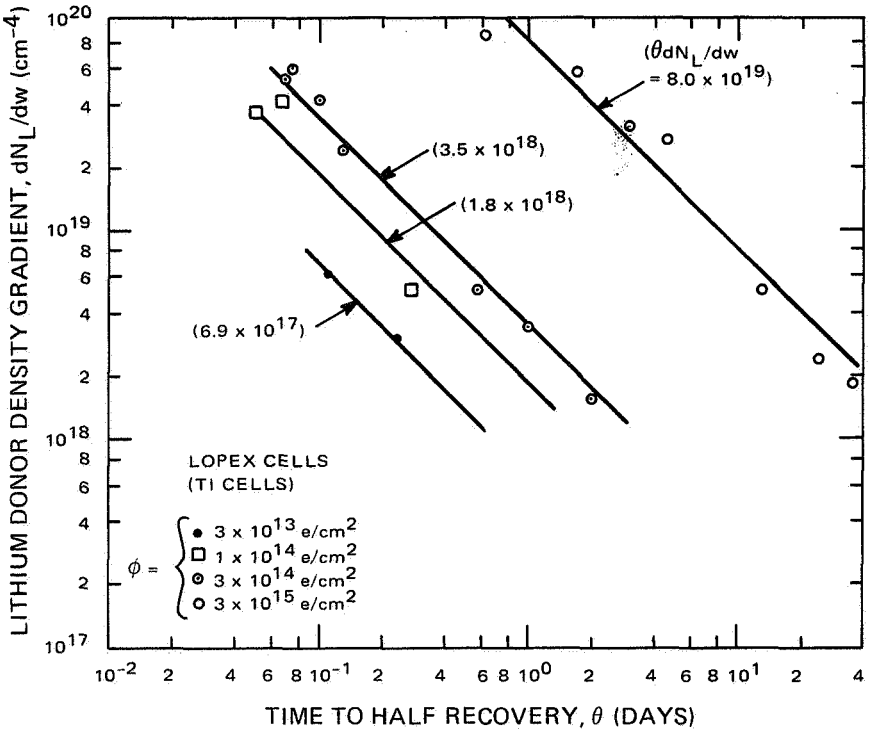

Figure 11. Time to Half Recovery at Room Temperature versus Lithium Gradient for Oxygen-Lean Texas Instruments Cells Irradiated to Fluences Ranging from 3×10^{13} to 3×10^{15} e/cm^2

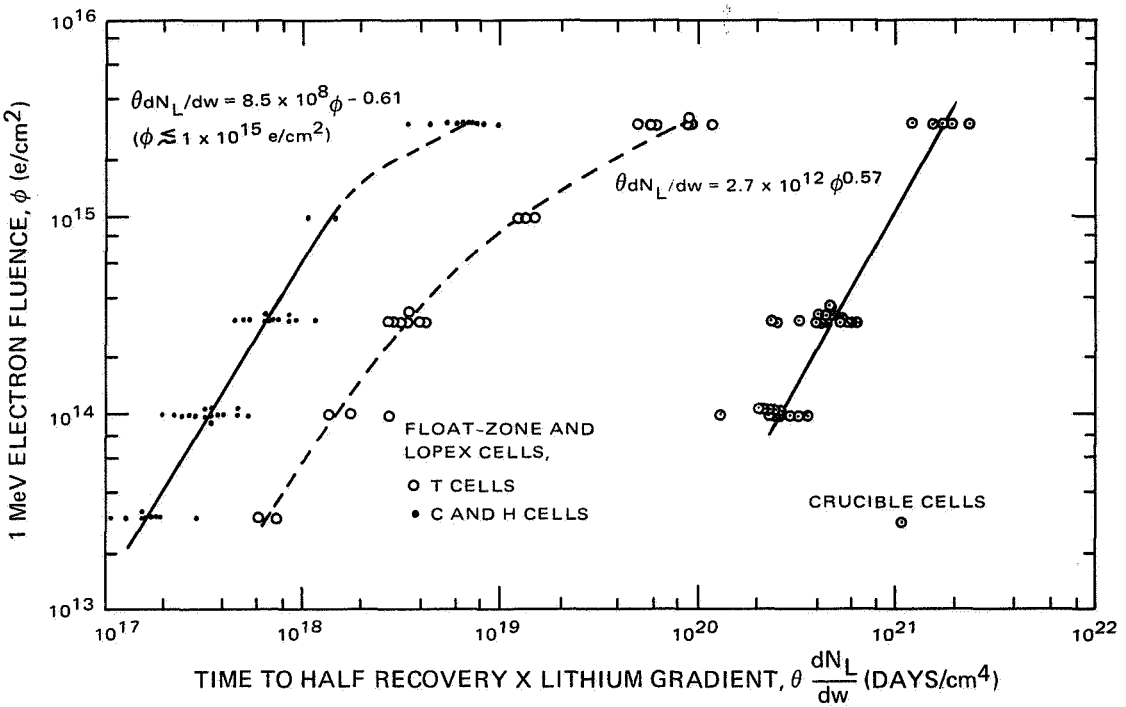

Figure 12. Product of Time to Half Recovery and Lithium Gradient, θ dN_L/dw Plotted versus 1 MeV Electron Fluence for Oxygen-Rich and Oxygen-Lean Lithium Cells

above 10^{15} e/cm^2. In the oxygen-rich cells the relation

$$\theta \, dN_L/dw = 2.7 \times 10^{12} \, \Phi^{0.57} \text{ days/cm}^4 \qquad (10)$$

provides a good approximation of cell recovery speed over the entire range of fluences.

E. LITHIUM DIFFUSION SCHEDULE AND DENSITY CONTROL

From the above and previous results, it is evident that many of the characteristics of lithium cells under electron irradiation can be predicted through knowledge of the lithium density gradient, dN_L/dw. Consequently, it is desirable to find relationships between this parameter and the fabrication parameters of the cell manufacturers. This has been accomplished for cell lots C13 (100 cells) and H3A (15 cells). Lot C13 consists of 10 groups of 10 cells, comprising 9 different lithium diffusion schedules with diffusion temperatures ranging from 330° C to 370° C and diffusion times from 3 to 7 hours. The lithium source was a lithium-in-oil suspension painted on the back surface of the cell. Figure 13 gives the distribution of lithium gradients measured for the cells in each of the 10 cell groups. There are five separate ordinates, each running from 1 to 10. The value of the ordinate at a given lithium gradient indicates the number of cells of that particular group with a lithium gradient greater than the value of the absicca. A pair of cell groups shares each ordinate since two groups were diffused at each lithium diffusion temperature. Each group is identified by a letter followed by a number in parentheses which gives the lithium diffusion time in hours. Several important factors are brought out in Figure 13: (1) for a given diffusion temperature, the shorter diffusion time gives a narrower gradient distribution; i.e., better gradient control; (2) the gradient distribution for the shorter diffusion time is always situated near the upper limit of that for the longer diffusion time; (3) at the highest diffusion temperature, even the short time diffusion shows a rather broad distribution; and (4) the average gradient (for short diffusion times) increases with diffusion temperature. Items (1), (2), and (3) indicate that as the diffusion time increases the lithium reservoir is somehow lost to the cell, either through lithium depletion or through interruption of the lithium-silicon interface. Therefore, for lithium introduction by the paint-on technique, the shortest practical diffusion time should be used.

A previously received cell lot, H3A, consisted of 15 quartz-crucible cells diffused with lithium for 8 hours at 325° C. Ten of the cells used a paint-on source; the other five, an evaporated lithium source. The cell distribution versus lithium gradient is shown in Figure 14. The cells using the paint-on source have a very broad distribution similar to those of the C13 cells using long diffusion times. The cells using an evaporated source, however, have a narrow distribution at the high end of the gradient scale. This supports the hypothesis of loss of the lithium source in the paint-on cells and also indicates that an evaporated source may provide the solution to this problem.

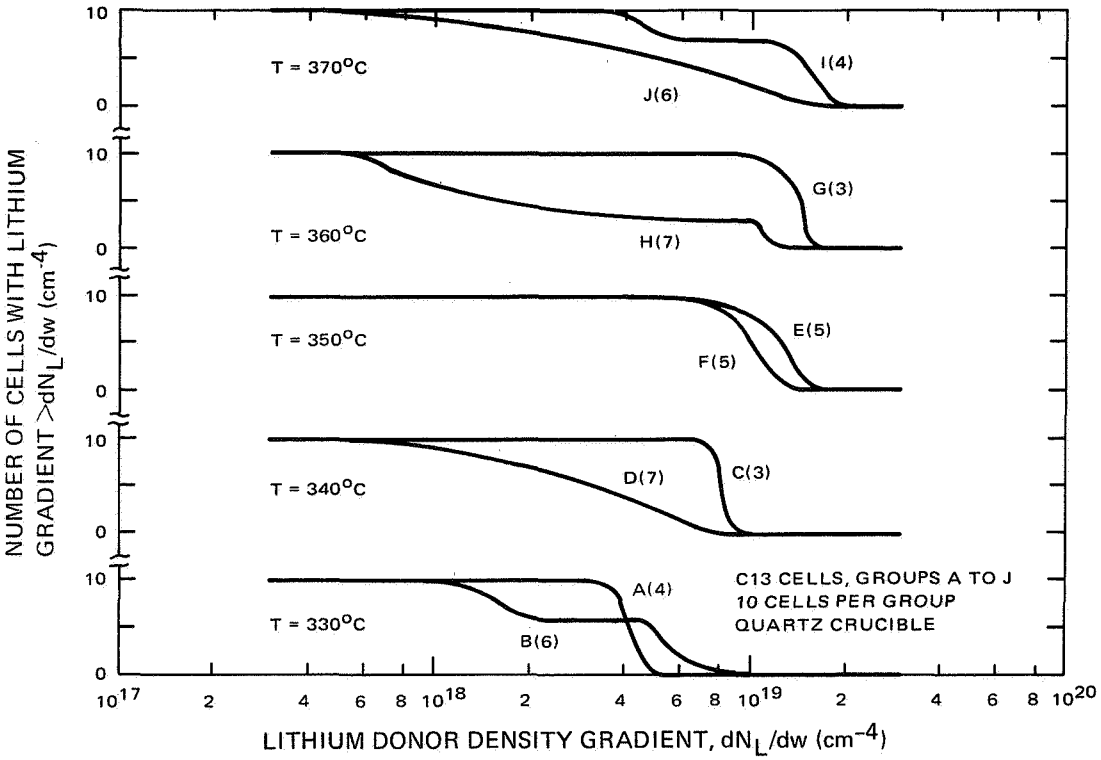

Figure 13. Distribution of Cells versus Lithium Gradient for the Ten Different Cell Groups Within Lot C13. Cell Groups are Identified by a Letter Followed by a Number in Parentheses Which Indicates the Duration of the Lithium Diffusion Cycle in Hours. Lithium Diffusion Temperatures are also Indicated

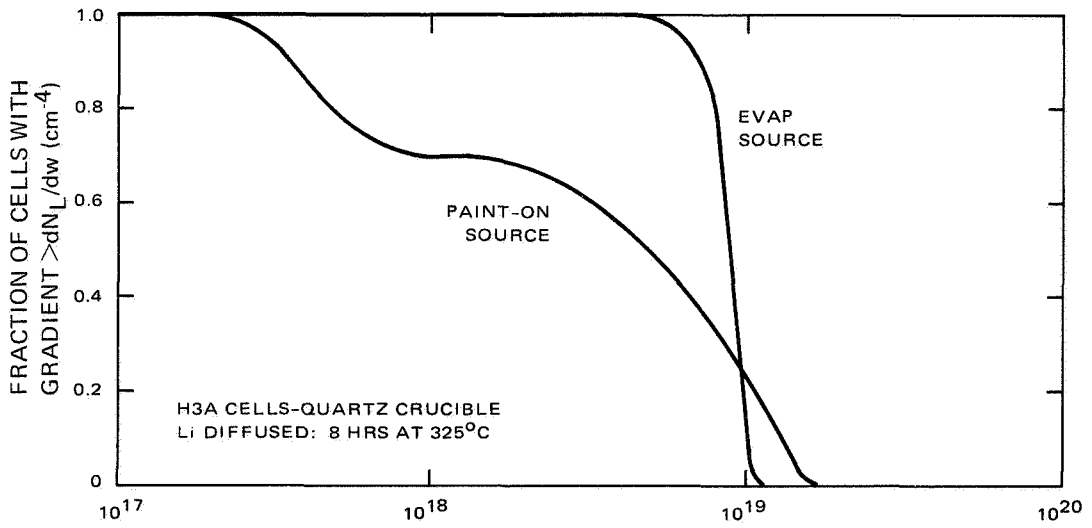

Figure 14. Distribution of Cells versus Lithium Gradient for H3A Cells Using Two Different Lithium Sources, Paint-On and Evaporated

SECTION III

CONCLUSIONS AND FUTURE WORK

A. PARAMETRIC STUDIES

Previous work has shown the lithium density gradient, dN_L/dw, obtained from reverse-bias capacitance measurements, to be a convenient and useful way to characterize the lithium density in a lithium cell by a single parameter. Work of the present reporting period has investigated the relationship between this physical parameter and the performance and recovery parameters of the lithium cell. Results show that knowledge of the lithium gradient enables the prediction of recovery speed for both oxygen-rich and oxygen-lean cells within a factor of approximately 2 for 1 MeV-electron fluences from 3×10^{13} to 3×10^{15} e/cm^2.

A relationship between the diffusion-length damage constant immediately after irradiation (before recovery) $K_L(O)$, the lithium gradient, dN_L/dw, and the electron fluence, Φ, has been obtained for C13 crucible cells:

$$K_L(O) = 5.3 \times 10^{-18} (dN_L/dw)^{1/2} (1 - 0.063 \log_{10} \Phi).$$

A check on previous post-irradiation data shows that this relationship also holds for H3A cells irradiated to 3×10^{14} e/cm^2. One additional relationship, that between the damage constant at peak recovery, $K_L(R)$, and dN_L/dw and ϕ, is required to complete the description of cell dynamics under electron irradiation. The C13 cells are now recovering, and this will be investigated upon completion of recovery.

These relations make it possible, in principle, to predict cell behavior in an electron environment using a simple non-destructive capacitance measurement. It is evident that a similar approach to predicting cell behavior under heavy particle irradiation should also be examined. However, caution must be exercised in making these predictions, as is illustrated by the C4 and C5 cells (previously identified as mavericks) which recovered at an anomalously rapid rate. It is thought that a set of general predictions based on lithium gradient can be generated for cells manufactured from silicon that is well-characterized.

Gradient measurements have also been correlated with lithium diffusion schedules. Results have shown that long diffusion times ($\geq$ 5 hours) with a paint-on source result in large cell-to-cell variations in gradient, probably due to a loss of the lithium source with time. The results also indicate that this problem can be overcome either by short diffusion times or by use of an evaporated lithium source.

It now appears that:

1. Capacitive measurements may provide a practical non-destructive quality control method for manufacturers and users of lithium cells.

2. Damage constants for lithium solar cells under electron bombardment are becoming sufficiently well-established that the predictions of cell performance and reliability in space electron environments are becoming a practical possibility. It is now time to extend this capability to the even more important proton-dominated regions of space.

Orbits that involve heavy proton damage include those to be used by the following vehicles:

1. TIROS weather satellites

2. Atmosphere Explorers

3. Elliptical MILCOMSATs

4. Spiral-trajectory spacecraft proceeding to geosynchronous orbit

5. Jupiter probes

Thus exploratory work on proton damage constants should be urgently provided along with confirmatory work on electron damage. Such work is proposed in the next section as a future add-on to the present technical effort.

B. FUTURE WORK

In the final quarter of the present contract, recovery and damage constant experiments will be continued on the C13 cells and on a set of non-lithium n/p control cells. Cells from the matrix requested in December 1970 will be radiation tested when received. The matrix of optimized cell parameters issued in the Fourth Quarterly Report will be updated to include all recent findings.

It is recommended that, in the future, add-on phases (not yet funded) of the study of proton damage constants of lithium cells begin; (2) that the quality-control potential of the capacitance method be extended; (3) and that capability to predict cell performance in space be extended in other ways.

REFERENCES

1. G. Brucker, T. Faith, J.P. Corra, and A. Holmes-Siedle, Fourth Quarterly Report, JPL Contract No. 952555. Prepared by RCA and issued July 10, 1970.

2. T. Faith, G. Brucker, and A. Holmes-Siedle, Sixth Quarterly Report, JPL Contract No. 952555. Prepared by RCA and issued Jan. 10, 1971, and T. Faith, J.P. Corra, and A. Holmes-Siedle, Conference Record of the Eighth Photovoltaic Spec. Conf., IEEE Catalog No. 70C 32 ED, 247 (1970).

3. G. Brucker, Phys, Rev. 183, 712 (1969).

RCA | Government and Commercial Systems | Astro Electronics Division | Princeton, New Jersey